Available online at www.sciencedirect.com

ScienceDirect

Nuclear Physics B 985 (2022) 116013

NUCLEAR PHYSICS B

www.elsevier.com/locate/nuclphysb

Di-photon decay of a light Higgs state in the BLSSM

Ahmed Ali Abdelalim [a,b,*], Biswaranjan Das [a,c], Shaaban Khalil [a], Stefano Moretti [d,e]

[a] *Center for Fundamental Physics, Zewail City of Science and Technology, 6 October City, Giza 12588, Egypt*
[b] *Physics Department, Faculty of Science, Helwan University, Cairo, Egypt*
[c] *East African Institute for Fundamental Research (ICTP-EAIFR), University of Rwanda, Kigali, Rwanda*
[d] *School of Physics and Astronomy, University of Southampton, Southampton, SO17 1BJ, United Kingdom*
[e] *Department of Physics and Astronomy, Uppsala University, Box 516, SE-751 20, Uppsala, Sweden*

Received 2 October 2022; accepted 28 October 2022
Available online 31 October 2022
Editor: Hong-Jian He

Abstract

In the context of the $B - L$ Supersymmetric Standard Model (BLSSM), we investigate the consistency of a scenario with a light Higgs boson with mass in the range $94 - 98$ GeV and a Standard Model (SM) Higgs state at 125 GeV with the results of a search performed by the CMS Collaboration in the di-photon channel primarily involving data at an integrated luminosity of 35.9 fb^{-1} and an energy of $\sqrt{s} = 13$ TeV. In this study, we present a Monte Carlo (MC) analysis of signal and background mimicking the experimental one and showing acceptable consistency with data, at both the integral and differential level.

1. Introduction

The discovery of a Higgs boson compatible with the one predicted by the Standard Model (SM), h, with a mass of 125 GeV, at the Large Hadron Collider (LHC) in July 2012, has been considered as the beginning of a new era in particle physics. This detection confirmed the Higgs mechanism of Electro-Weak Symmetry Breaking (EWSB) generating masses for fundamental

* Corresponding author.
E-mail addresses: aabdelalim@zewailcity.edu.eg (A.A. Abdelalim), bdas@zewailcity.edu.eg (B. Das), skhalil@zewailcity.edu.eg (S. Khalil), S.Moretti@soton.ac.uk, stefano.moretti@physics.uu.se (S. Moretti).

https://doi.org/10.1016/j.nuclphysb.2022.116013

particles. It also boosted the expectation of discovering New Physics (NP) Beyond the SM (BSM), as we also know that for the aforementioned mass value, the SM is incomplete, showing flaws both theoretically and experimentally [1,2]. Many of these (e.g., the hierarchy problem, the absence of coupling unification, an insufficient matter-antimatter asymmetry, the lack of a dark matter candidate, unexplained neutrino oscillations, etc.) can however be remedied by Supersymmetry (SUSY), although the latter has itself drawbacks, e.g., the $\mu-$problem, even if consistent with both collider and Dark Matter (DM) data, when formulated in its minimal version, the so-called Minimal Supersymmetric Standard Model (MSSM) [3]. However, non-minimal realisations of SUSY, e.g., with an enlarged gauge and/or Higgs sector, are both theoretically plausible and better compatible with experimental data [1].

The statistically most significant channel leading to the 2012 signal emerged in the $gg \to h \to \gamma\gamma$ production and decay mode, primarily thanks to the high experimental resolution that can be achieved (in the invariant mass of the two photons, $M_{\gamma\gamma}$) via the di-photon final state. Hence, it is not surprising that this channel is being routinely used by ATLAS and CMS in their search for additional (neutral) Higgs bosons, an endeavour that has indeed started immediately after the aforementioned discovery, since most BSM scenarios (Supersymmetric and not) predict the existence of extra neutral Higgs states. The possibility of the existence of the latter, lighter or heavier than the SM state, is thus an open and challenging phenomenological problem.

The CMS collaboration has recently found potential signals for another neutral Higgs boson, h', with a mass of 94 to 98 GeV, precisely in the discussed gluon-fusion initiated channel leading to the di-photon final state, i.e., $gg \to h' \to \gamma\gamma$. The corresponding data were collected at Center-of-Mass (CM) energies of $\sqrt{s} = 8$ and 13 TeV and integrated luminosities of 19.7 and 35.9 fb^{-1}, respectively[1] [4]. Based on these data, the CMS collaboration observed a resonant structure at $94 - 98$ GeV in the $M_{\gamma\gamma}$ spectrum with a local (global) significance of 2.8 (1.3) standard deviations, respectively.[2] Despite the fact that this hint for a new resonance is still rather preliminary, while waiting for the full data set of Run 2 and beyond, it gained considerable attention in the particle physics community and several BSM explanations for it have already been proposed in the context of both SUSY [5] and non-SUSY models [6]. If these observations are confirmed by future data, it will be a significant direct evidence of NP, whichever the origin of it.

In the present paper we show that a specific extension of the MSSM, the aforementioned BLSSM [7], which has a rich Higgs sector consisting of two Higgs doublets and two Higgs singlets, can accommodate the observed anomaly. In particular, we emphasise that one of the CP-even Higgs bosons of this BSM construct can act as the potential h' state behind the aforementioned excess in $M_{\gamma\gamma}$, with the model still providing a SM-like Higgs state with 125 GeV, thus compatible with current LHC measurements. The BLSSM is an extension of the MSSM obtained by adopting an additional $U(1)_{B-L}$ gauge group, i.e., the full gauge structure is $SU(3)_C \times SU(2)_L \times U(1)_Y \times U(1)_{B-L}$. This model contains three SM singlet chiral superfields $\widehat{N}_{1,2,3}$ (yielding right-handed neutrinos), two SM singlet chiral Higgs superfields $\widehat{\chi}_{1,2}$ (providing three additional physical Higgs states) and the $\widehat{Z}'$ vector superfield associated with the $U(1)_{B-L}$ gauge boson (embedding a physical Z' state), in addition to the MSSM superfields. Interestingly, it was shown that the scale of $B - L$ symmetry breaking is related to the soft SUSY-breaking scale [10], so that it is not unreasonable to find that this model can predict right-handed neutri-

[1] Note that the ATLAS collaboration has also published its analysis with 80 fb^{-1} data at 13 TeV in the di-photon channel in the mass range 65 – 110 GeV with no significant excess over the SM expectation [8].

[2] Similar observation had been made at LEP 2 for a scalar mass ~ 98 GeV with an excess of 2.3σ local significance in the $b\bar{b}$ channel [9].

nos, Z' and Higgs states at or even below the TeV scale. This is in particular true when the low energy spectrum is generated by starting from a Grand Unification Theory (GUT) formulation, which is our approach here.

The mixing between the SM-like Higgs state h and the BLSSM-specific Higgs state h' is proportional to the gauge coupling of the gauge kinetic mixing $\widetilde{g}$ between the Z and Z', which is (in a non-universal description) a free parameter and can be of order of 0.5. In this case, a large Higgs mixing is generated, which yields significant couplings between the h' and SM fermions and gauge bosons. Therefore, the production and decay rates of the h' state are not generally suppressed, including in the $gg \to h' \to \gamma\gamma$ channel [11], which proceeds mainly via top quark and $W^{\pm}$ gauge boson loops at production and decay level, respectively. Hence, the BLSSM can account for the observed $94 - 98$ GeV potential signal.

The paper is organised as follows. In Sec. 2, we describe the Higgs sector of the BLSSM and emphasise that the mass of the lightest CP-even Higgs boson can naturally be around $94 - 98$ GeV with also a SM-like Higgs state having a mass of 125 GeV. In Sec. 3, we investigate the would be BLSSM signal in the $gg \to h' \to \gamma\gamma$ channel and show that it can explain the excess presently observed by the CMS collaboration as well as offer a chance for h' discovery already with the full Run 2 data set. Our conclusions are presented in Sec. 4.

2. The BLSSM Higgs sector

The BLSSM superpotential is given by

$$\begin{aligned} W_{\rm BLSSM} = {} & y_u \widehat{Q}\widehat{H}_2\widehat{U}^c + y_d \widehat{Q}\widehat{H}_1\widehat{D}^c + y_e \widehat{L}\widehat{H}_1\widehat{E}^c \\ & + \mu \widehat{H}_1\widehat{H}_2 + y_\nu \widehat{L}\widehat{H}_2\widehat{N}^c + y_N \widehat{N}^c\widehat{\chi}_1\widehat{N}^c \\ & + \mu' \widehat{\chi}_1\widehat{\chi}_2 \,, \end{aligned} \tag{1}$$

where the first four terms are the usual MSSM ones, the next two terms represent the Yukawa interactions of the known neutrinos and between the additional right-handed ones N_i ($i = 1, 2, 3$) and the singlet Higgs field χ_1, respectively. The last term represents the bilinear mixing between χ_1 and χ_2 while y_u, y_d, y_e and y_ν are the quark, lepton and neutrino Yukawa coupling constants, respectively. Furthermore, y_N is the Yukawa coupling constant between N_i and χ_1, Q and L are the left-handed quark and lepton doublet superfields while U, D and E are the right-handed up-type, down-type and electron-type singlet ones, respectively. The charge conjugation is denoted by the superscript c. Then, H_1 and H_2 are the $SU(2)_L$ Higgs doublet superfields with opposite hypercharge $Y = \pm 1$.

One obtains the masses of the physical neutral BLSSM Higgs states in terms of the Higgs fields,

$$\begin{aligned} H^0_{1,2} &= \frac{1}{\sqrt{2}}(v_{1,2} + \sigma_{1,2} + i\phi_{1,2}) \,, \\ \chi^0_{1,2} &= \frac{1}{\sqrt{2}}(v'_{1,2} + \sigma'_{1,2} + i\phi'_{1,2}) \,, \end{aligned} \tag{2}$$

where the real and imaginary parts correspond to the CP-even (or scalar) and the CP-odd (or pseudoscalar) Higgs states. Here, $v_{1,2}$ and $v'_{1,2}$ are the Vacuum Expectation Values (VEVs) of the Higgs fields $H_{1,2}$ and $\chi_{1,2}$, respectively. The CP-odd neutral Higgs mass-squared matrix at the tree-level in the basis $(\phi_1, \phi_2, \phi'_1, \phi'_2)$ is given by

$$\mathcal{A}^2 = \begin{pmatrix} B_\mu \tan\beta & B_\mu & 0 & 0 \\ B_\mu & B_\mu \cot\beta & 0 & 0 \\ 0 & 0 & B_{\mu'} \tan\beta' & B_{\mu'} \\ 0 & 0 & B_{\mu'} & B_{\mu'} \cot\beta' \end{pmatrix}, \tag{3}$$

with

$$\begin{aligned} B_\mu &= -\frac{1}{8}\left\{-2\widetilde{g} g_{BL} v'^2 \cos 2\beta' + 4M_{H_1}^2 - 4M_{H_2}^2 + (g_1^2 + \widetilde{g}^2 + g_2^2) v^2 \cos 2\beta\right\} \tan 2\beta\,, \\ B_{\mu'} &= -\frac{1}{4}\left(-2g_{BL}^2 v'^2 \cos 2\beta' + 2M_{\chi_1}^2 - 2M_{\chi_2}^2 + \widetilde{g} g_{BL} v^2 \cos 2\beta\right) \tan 2\beta'\,, \end{aligned} \tag{4}$$

where $\tan\beta = \frac{v_2}{v_1}$ and $\tan\beta' = \frac{v_2'}{v_1'}$. Here, g_{BL} is the gauge coupling constant of $U(1)_{B-L}$ and $\widetilde{g}$ is the gauge coupling constant of the mixing between $U(1)_Y$ and $U(1)_{B-L}$. Finally, g_1 and g_2 are the $U(1)_Y$ and $SU(2)_L$ gauge coupling constants, respectively.

The CP-even neutral Higgs mass-squared matrix at the tree-level in the basis $(\sigma_1, \sigma_2, \sigma_1', \sigma_2')$ is given by

$$\mathcal{M}^2 = \begin{pmatrix} \mathcal{M}_{hH}^2 & \mathcal{M}_{hh'}^2 \\ \left(\mathcal{M}_{hh'}^2\right)^T & \mathcal{M}_{h'H'}^2 \end{pmatrix}, \tag{5}$$

where $\mathcal{M}_{hH}$ is the MSSM CP-even mass matrix which results into a SM-like Higgs boson h with a mass $m_h \sim 125$ GeV and a heavy Higgs boson H with a mass $m_H \sim \mathcal{O}(1\text{ TeV})$ at the one-loop level, with the mass eigenvalues at the tree-level given by

$$m_{h,H}^2 = \frac{1}{2}\left\{m_A^2 + m_Z^2 \mp \sqrt{(m_A^2 + m_Z^2)^2 - 4m_A^2 m_Z^2 \cos^2 2\beta}\right\}. \tag{6}$$

The BLSSM mass matrix $\mathcal{M}_{h'H'}$ reads

$$\mathcal{M}_{h'H'}^2 = \begin{pmatrix} m_{A'}^2 c_{\beta'}^2 + g_{BL}^2 v_1'^2 & -\frac{1}{2}m_{A'}^2 s_{2\beta'} - g_{BL}^2 v_1' v_2' \\ -\frac{1}{2}m_{A'}^2 s_{2\beta'} - g_{BL}^2 v_1' v_2' & m_{A'}^2 s_{\beta'}^2 + g_{BL}^2 v_2'^2 \end{pmatrix} \tag{7}$$

with $c_x = \cos x$ and $s_x = \sin x$. The eigenvalues of this matrix at the tree-level can be given as

$$m_{h',H'}^2 = \frac{1}{2}\left\{m_{A'}^2 + m_{Z'}^2 \mp \sqrt{(m_{A'}^2 + m_{Z'}^2)^2 - 4m_{A'}^2 m_{Z'}^2 \cos^2 2\beta'}\right\}. \tag{8}$$

The matrix $\mathcal{M}_{hh'}$ can be denoted as

$$\mathcal{M}_{hh'}^2 = \frac{1}{2}\widetilde{g} g_{BL} \begin{pmatrix} v_1 v_1' & -v_1 v_2' \\ -v_2 v_1' & v_2 v_2' \end{pmatrix}. \tag{9}$$

The CP-even physical Higgs mass states can be obtained by diagonalising the Higgs mass-squared matrix given by Eq. (5) with a unitary matrix $\mathcal{R}$ as

$$\mathcal{R}\mathcal{M}^2\mathcal{R}^\dagger = \text{diag}\{m_h^2, m_{h'}^2, m_H^2, m_{H'}^2\}. \tag{10}$$

In order to find solutions consistent with the CMS observation of a scalar of mass around 94 – 98 GeV [4], we perform a parameter space scan in the BLSSM with an in-house scanning tool which calls `SPheno-v4.0.4` [12] to generate the particle spectrum with two-loop corrected

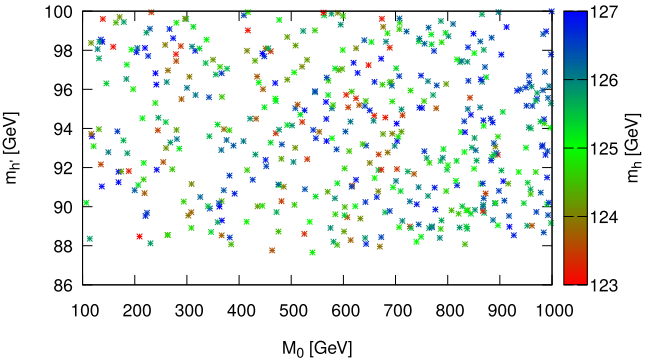

Fig. 1. Scan of $m_{h'}$ vs M_0 with m_h on the colour map.

Higgs masses for each randomly scanned parameter space point. `SPheno` requires the model files to generate the output spectrum in the context of a particular model (in our case it is the BLSSM) for a given point. These model files are generated with the public package `SARAH-v4.14.3` [13]. We perform the scan at the GUT scale by varying four input parameters, namely, the universal Soft SUSY-Breaking (SSB) scalar mass term M_0 ($= M_{Q_{1,2,3}} = M_{U_{1,2,3}} = M_{D_{1,2,3}} = M_{L_{1,2,3}} = M_{E_{1,2,3}}$) over 100 – 1000 GeV, the universal SSB gaugino mass term $M_{1/2}$ ($= 2M_1 = M_2 = \frac{1}{3}M_3$) over 1000 – 4500 GeV, $\tan\beta$ over 1 – 60 and the universal Higgs to sfermion trilinear coupling A_0 ($= A_{\tilde{t}} = A_{\tilde{b}} = A_{\tilde{\tau}}$) over 1000 – 4000 GeV, while keeping $m_{Z'}$ and $\tan\beta'$ fixed at 2500 GeV and 1.15, respectively.

The randomly scanned points are required to produce the lightest neutral Higgs boson mass in the range 94 GeV $\leq m_{h'} \leq$ 98 GeV (approximately). As far as the experimental constraints are concerned, these points should also result in a SM-like Higgs boson with a mass m_h, which allows ± 2 GeV uncertainty in its theoretical model prediction, consistent with the experimental measurement of $m_h = 125.09 \pm 0.32$ GeV [14]. The points are then run through `HiggsBounds-v5.9.1` [15] and `HiggsSignals-v2.6.1` [16]. HiggsBounds checks the theoretical prediction of a model with an extended Higgs sector against the exclusion bounds on cross section at 95% CL obtained from the Higgs search experiments at LEP, Tevatron and the LHC. It selects the search channel with highest statistical sensitivity for each Higgs state in the model by using the expected exclusion limit on the cross section. Comparing the model prediction for each Higgs boson with the observed limit for that particular channel, a parameter space point is excluded if the predicted signal strength exceeds the observed limit for any of the Higgs bosons present in that model. On the other hand, HiggsSignals performs a χ^2-fit of the signal strengths of the observed Higgs boson (at 125 GeV) for a given model point against the LHC measurements, and rules it out if $\Delta\chi^2 = \chi^2_{\text{model}} - \chi^2_{\text{SM}} > 6.18$ (assuming a 2σ Gaussian error on the best-fit value). `SPheno` also calculates flavour observables, so that the scanned points are also asked to satisfy the experimental constraints on the Branching Ratios (BRs) of the most stringent B-meson decay channels within a 2σ error, which are given by $\text{BR}(B \to X_s\gamma) = (3.32 \pm 0.15) \times 10^{-4}$, $\text{BR}(B_s \to \mu^+\mu^-) = (3.1 \pm 0.6) \times 10^{-9}$ and $\text{BR}(B_u \to \tau^\pm\nu_\tau) = (1.06 \pm 0.19) \times 10^{-4}$ [17], respectively.

In Fig. 1 we present the randomly scanned points on the $M_0 - m_{h'}$ plane where the colour map represents the values of m_h for those points. It shows that below 1000 GeV almost all values of M_0 are allowed in the chosen BLSSM scenario which can accommodate a light scalar of mass $94 - 98$ GeV and a SM-like scalar with a mass near 125 GeV at the same time. Similarly, Fig. 2

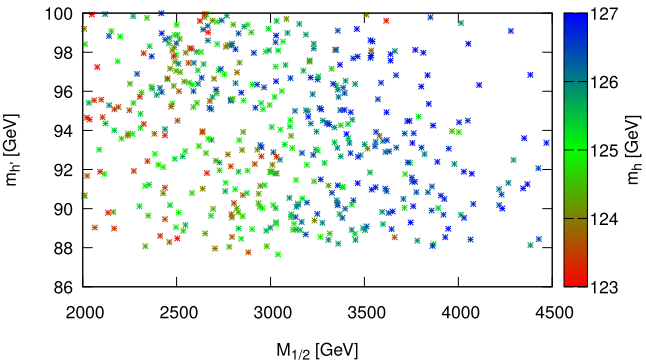

Fig. 2. Scan of $m_{h'}$ vs $M_{1/2}$ with m_h on the colour map.

depicts the scanned points on the $M_{1/2} - m_{h'}$ plane while the values of m_h are given by the colour map. It shows that the points with $M_{1/2} < 2000$ GeV are excluded as moderately heavy charginos and neutralinos ($\sim$1000 GeV) are required to reach the aforementioned limits on the masses of the Higgs bosons. Altogether, there exists a sizeable region in the BLSSM parameter space, when M_0 is somewhat lighter than 1000 GeV, $M_{1/2}$ lies between 2000 and 4000 GeV and $A_0 > 3500$ GeV, wherein this particular mass configuration is realised without excessive fine tuning, as all the scanned points are equally viable in the light of latest experimental constraints from collider searches for BSM and the SM-like Higgs bosons as well as all relevant flavour physics constraints.

In the next section, we present our Monte Carlo (MC) analysis in the light of the CMS observation of a light scalar in terms of a few Benchmark Points (BPs) selected from our random scan. The specific values of the input parameters associated with these BPs are listed in Table 1. Furthermore, the Higgs masses and the cross sections for the BPs are presented in Table 2, where we have also reported the values of the corresponding signal strengths $\mu_{h'}$ and μ_h, i.e., the ratios $\frac{\sigma(pp\to h'\to\gamma\gamma)}{\sigma(pp\to h'_{\rm SM}\to\gamma\gamma)}$ and $\frac{\sigma(pp\to h\to\gamma\gamma)}{\sigma(pp\to h_{\rm SM}\to\gamma\gamma)}$ where $h'_{\rm SM}$ and $h_{\rm SM}$ are the SM-like states with masses equal to $m_{h'}$ and m_h, respectively, illustrating that our h' state is always significantly weakly coupled to gluons and photons. Note that the tabulated cross sections (given at 13 TeV) are calculated with the public package `MadGraph5-v1.5.1` [18], which is also used for our (irreducible) background, i.e., $q\bar{q}, gg \to \gamma\gamma$.[3] The ensuing Leading Order (LO) results are supplemented by inclusive k-factors for both signals and background, as follows. We consider the Next-to-LO (NLO) k-factor which is defined as $k_{\rm NLO} = \frac{\sigma_{\rm NLO}}{\sigma_{\rm LO}}$. For the signal, in order to estimate $k_{\rm NLO}$, we calculate $\sigma(gg \to h, h')$ at the LO and NLO using the public code `SusHi-v1.7.0` [19], since the largest higher order corrections are only associated with the production process. Here, the value of $k_{\rm NLO}$ is essentially 2.4 in the entire mass range $94 - 125$ GeV. For the background, we assume a constant $k_{\rm NLO} = 1.3$ in our analysis following Ref. [20].

In Table 3 we present the Higgs effective couplings to gauge bosons, namely, the photon, gluon and the W boson, normalised to their corresponding SM values for h' and h, i.e., $k_{AA} = \frac{g^{\rm BLSSM}_{XAA}}{g^{\rm SM}_{XAA}}$, where $X = h', h$ and $A = \gamma, g, W$, for the selected BPs. The last three columns

[3] As the majority of the excess in the CMS analysis comes from the higher energy data, henceforth, we neglect benchmarking against the 8 TeV ones.

Table 1
The values of the input parameters associated with the selected BPs. M_0, $M_{1/2}$, A_0, μ, μ' are in the units of GeV and B_μ, $B_{\mu'}$ are in the units of GeV^2.

BP	M_0	$M_{1/2}$	tanβ	A_0	μ	μ'	B_μ	$B_{\mu'}$
1	998	2141	29.9	3837	1849	2020	1.5×10^5	5.2×10^6
2	961	2370	15.3	3748	2019	1901	4.4×10^5	5.0×10^6
3	995	2411	15.6	3739	2046	1932	4.5×10^5	5.2×10^6
4	146	3351	44.7	3736	2739	1162	1.4×10^5	3.7×10^6
5	874	2450	11.4	3709	2092	1770	6.4×10^5	4.5×10^6

Table 2
The masses (in GeV) of the two lightest neutral Higgs bosons and the cross sections (in fb) at 13 TeV for the processes $pp \to h' \to \gamma\gamma$ and $pp \to h \to \gamma\gamma$ for the selected BPs. The last two columns show the corresponding $\mu_{h'}$ and μ_h values, as defined in the text.

BP	$m_{h'}$	m_h	$\sigma(pp \to h' \to \gamma\gamma)$	$\sigma(pp \to h \to \gamma\gamma)$	$\mu_{h'}$	μ_h
1	95.3	125.9	13.1	43.5	0.37	1.12
2	96.1	125.9	13.2	43.8	0.37	1.13
3	96.2	126.1	13.5	43.4	0.38	1.12
4	96.3	125.4	10.0	49.0	0.28	1.26
5	96.6	125.3	13.0	44.7	0.37	1.15

Table 3
Values of normalised Higgs couplings (see the text) to gauge bosons and the corresponding BRs for h' and h for the selected BPs.

X	$k_{\gamma\gamma}$	k_{gg}	k_{WW}	BR$_{\gamma\gamma}$	BR$_{\rm gg}$	BR$_{\rm WW}$
h'	0.529	0.478	0.463	2.199×10^{-3}	7.633×10^{-2}	3.493×10^{-3}
h	1.019	0.888	0.886	3.290×10^{-3}	8.229×10^{-2}	2.865×10^{-1}
h'	0.531	0.478	0.463	2.262×10^{-3}	7.747×10^{-2}	4.447×10^{-3}
h	1.021	0.888	0.886	3.311×10^{-3}	8.245×10^{-2}	2.872×10^{-1}
h'	0.536	0.482	0.467	2.267×10^{-3}	7.753×10^{-2}	4.496×10^{-3}
h	1.019	0.885	0.884	3.308×10^{-3}	8.203×10^{-2}	2.925×10^{-1}
h'	0.461	0.411	0.399	2.323×10^{-3}	7.802×10^{-2}	4.791×10^{-3}
h	1.075	0.919	0.917	3.440×10^{-3}	8.307×10^{-2}	2.818×10^{-1}
h'	0.524	0.471	0.457	2.294×10^{-3}	7.807×10^{-2}	5.054×10^{-3}
h	1.025	0.891	0.890	3.329×10^{-3}	8.338×10^{-2}	2.762×10^{-1}

represent the corresponding BRs for the $\gamma\gamma$, gg and WW decay modes of h' and h. Similarly, the effective couplings to SM fermions, namely, the b quark, μ and the τ leptons, normalised to their corresponding SM values for h' and h, i.e., $k_{BB} = \frac{g^{\rm BLSSM}_{XBB}}{g^{\rm SM}_{XBB}}$, where $B = b, \mu, \tau$, are listed in Table 4. The corresponding BRs are represented by the last three columns. Assuming that the gluon fusion mode dominates the h' and h production at the LHC, we note that the corresponding signal strengths $\mu_{h'}$ and μ_h in the di-photon decay channel can be approximated to $k^2_{gg} \times \frac{\rm BR_{\gamma\gamma}}{\rm BR^{SM}_{\gamma\gamma}}$, showing a good agreement with the values listed in Table 2. Moreover, the tabulated values of μ_h are also consistent with the experimental result reported by the CMS collaboration for the

Table 4
Values of normalised Higgs couplings (see the text) to SM fermions and the corresponding BRs for h' and h for the selected BPs.

X	$k_{bb} = k_{\mu\mu} = k_{\tau\tau}$	BR_{bb}	$BR_{\mu\mu}$	$BR_{\tau\tau}$
h'	0.464	7.922×10^{-1}	3.042×10^{-4}	8.774×10^{-2}
h	0.891	5.178×10^{-1}	2.084×10^{-4}	6.015×10^{-2}
h'	0.464	7.902×10^{-1}	3.039×10^{-4}	8.766×10^{-2}
h	0.890	5.170×10^{-1}	2.081×10^{-4}	6.006×10^{-2}
h'	0.468	7.901×10^{-1}	3.039×10^{-4}	8.765×10^{-2}
h	0.887	5.122×10^{-1}	2.062×10^{-4}	5.952×10^{-2}
h'	0.399	7.893×10^{-1}	3.037×10^{-4}	8.759×10^{-2}
h	0.920	5.220×10^{-1}	2.099×10^{-4}	6.060×10^{-2}
h'	0.458	7.891×10^{-1}	3.038×10^{-4}	8.761×10^{-2}
h	0.892	5.269×10^{-1}	2.119×10^{-4}	6.116×10^{-2}

$\gamma\gamma$ channel (Run 2 data at 13 TeV and 35.9 fb^{-1}), which is given by $1.18^{+0.17}_{-0.14}$ [21]. Altogether then, the k-factors and the BRs are such that the SM state has signal strengths compatible with the LHC discovery data while the BLSSM one is compatible with the $\mu_{h'}$ values given in Table 2 (through the h' width), signalling their overall consistency with the LHC exclusion limits. Note that `HiggsBounds and HiggsSignals` have already checked the consistency of each of the Higgs states in the light of latest exclusion limits on their cross section and signal strength measurements reported by the LHC justifying our selection of BPs.

3. Numerical analysis and results

In our analysis, we selected all events that contain a di-photon pair in the detector fiducial range $|\eta^{\gamma}| \leqslant 2.5$ and out of the crack region between the barrel and end-cap parts of the CMS Electro-Magnetic (EM) calorimeters. Each photon in the pair has to satisfy a requirement on the ratio of its $p_T^{\gamma_i}$ ($i = 1, 2$, with 1 (2) being the most (least) energetic one) value to the invariant mass of the di-photon system. These requirements are: $p_T^{\gamma_1}/M_{\gamma\gamma} > 30.6/65.0 = 0.47$ and $p_T^{\gamma_2}/M_{\gamma\gamma} > 18.2/65.0 = 0.28$. Our results are therefore directly comparable to the CMS class0 data of [4], which apply the same requirements on the di-photon system. We have digitised such data (see black cross symbols thereafter). Figs. 3–7 show the $M_{\gamma\gamma}$ distribution for the aforementioned CMS data (at 13 TeV) alongside the MC ones for our BP1–5, where yellow markers refer to the h' signal, pink markers refer to the h signal while red markers refer to the SM background (the former two being stacked onto the latter). In Figs. 3–7, we see moderate peaks (the yellow markers in the zoomed-in panels) stemming from the background for the h' signals around 95 or 96 GeV (depending on the BP). These peaks can be clearly seen in Fig. 8, which has finer binning (0.1 GeV), clearly beyond the scope of current detector performance, yet confirming that improvements to the $\gamma\gamma$ mass resolution would greatly help to reveal these potential signals. Moreover, clear peaks are shown around 125 GeV which are consistent with the SM Higgs boson, h. To convince oneself of the statistical relevance of both Higgs boson peaks, we present in Table 5 a comparison between the number of events from each signal and background. We used the number of events in the di-photon mass range $94 - 100$ GeV to calculate the significance for BP1–5. This has been calculated using the formula $S/\sqrt{B}$, where S is the number of h' events

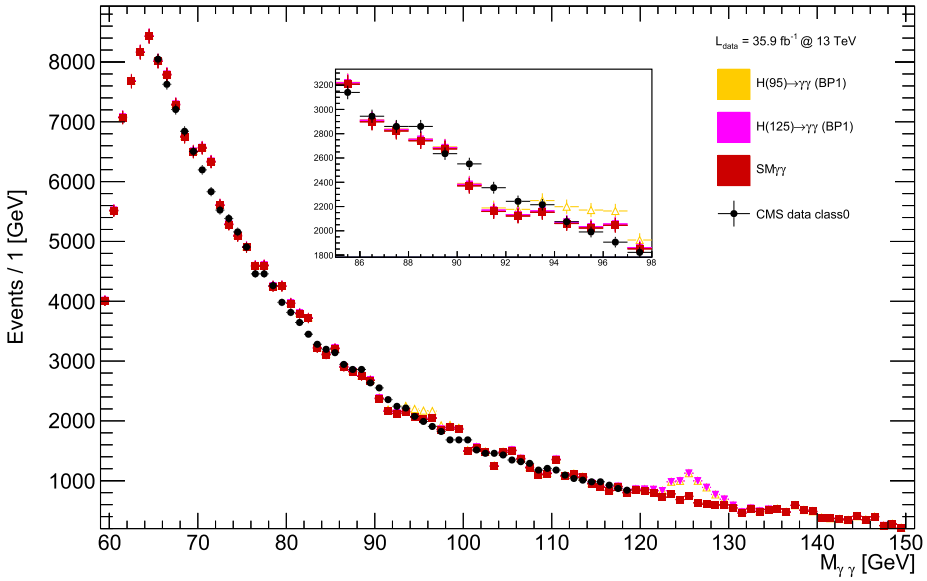

Fig. 3. BP1 versus CMS data at 13 TeV [4]. Yellow points represent $h' \to \gamma\gamma$, pink points represent $h \to \gamma\gamma$ while red points show the SM background.

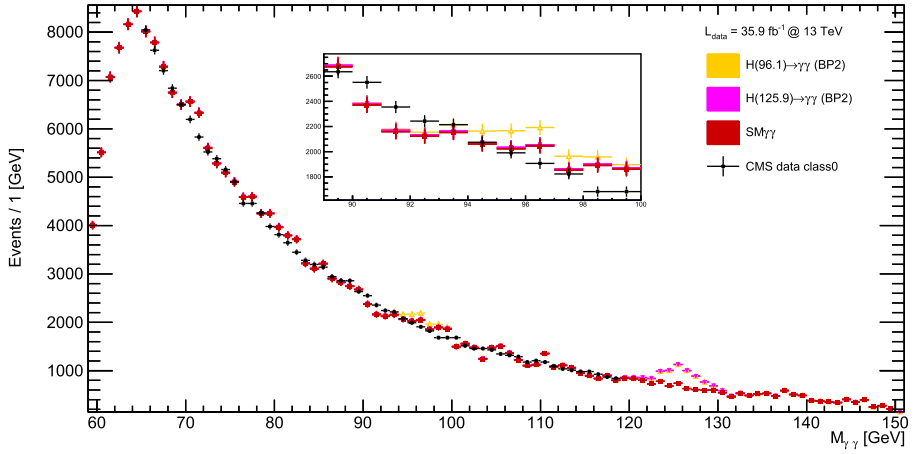

Fig. 4. BP2 versus CMS data at 13 TeV [4]. Yellow points represent $h' \to \gamma\gamma$, pink points represent $h \to \gamma\gamma$ while red points show the SM background.

and B is that of background ones. Herein, it is clear that there is not a perfect overlap between the events that our BPs produce and the size of the excess found by CMS. However, we would like to emphasise that the latter was our estimate obtained through digitising software, which we deem to consequently be not very accurate either. In short, we have provided the numbers in Table 5 primarily to convey the message that there is a sizeable region over the BLSSM parameter space where there is potential to explain the CMS anomalous events.

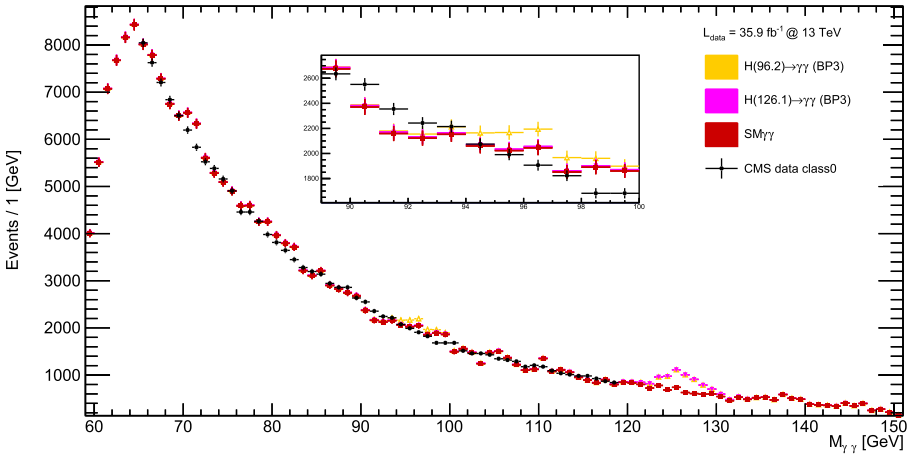

Fig. 5. BP3 versus CMS data at 13 TeV [4]. Yellow points represent $h' \to \gamma\gamma$, pink points represent $h \to \gamma\gamma$ while red points show the SM background.

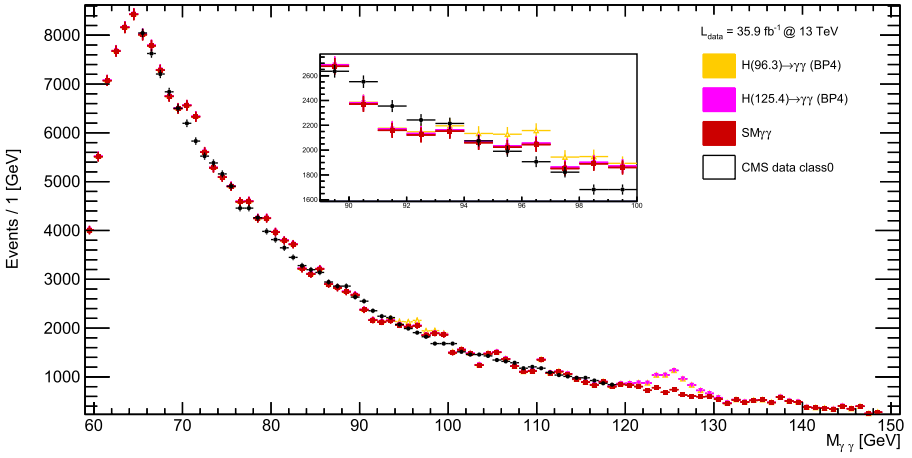

Fig. 6. BP4 versus CMS data at 13 TeV [4]. Yellow points represent $h' \to \gamma\gamma$, pink points represent $h \to \gamma\gamma$ while red points show the SM background.

Finally, Fig. 9 shows the integrated luminosity needed to discover the h' state of the BLSSM in di-photon events using CMS data at 13 TeV for our five BPs. It is clear that, for all of our BPs, the discovery is within reach of Run 2, as luminosity values of 57(71)[71]{87}[84] fb^{-1} are needed to reach a 5σ excess in the $94-98$ GeV region for BP1(2)[3]{4}[5].

4. Conclusions

Motivated by a $\sim 2.8\sigma$ excess recorded by the CMS experiment in the di-photon channel at the integrated luminosity of 35.9 fb^{-1} at $\sqrt{s} = 13$ TeV (in fact, with a moderate contribution from 8 TeV data too) around a mass of order $94-98$ GeV, we have analysed the discovery potential of a light neutral Higgs boson h' available in the context of the BLSSM at Run 2 of the LHC. We

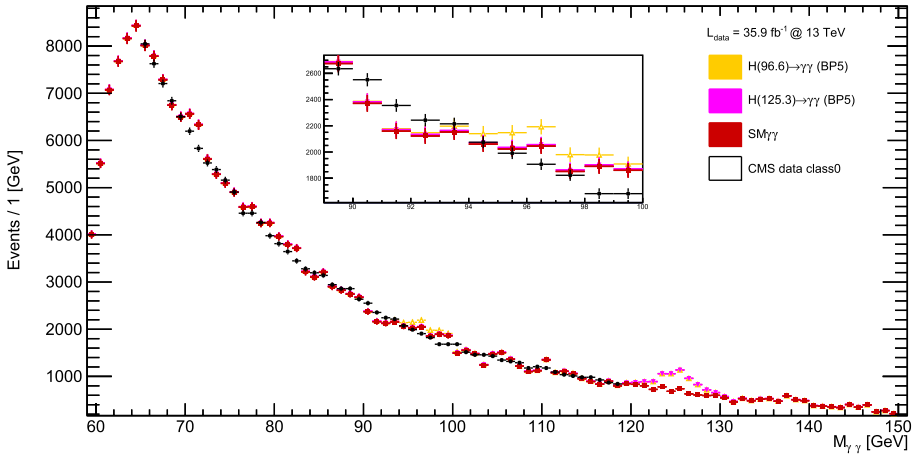

Fig. 7. BP5 versus CMS data at 13 TeV [4]. Yellow points represent $h' \to \gamma\gamma$, pink points represent $h \to \gamma\gamma$ while red points show the SM background.

Table 5
Number of events in the CMS data of [4] and our MC samples in different $M_{\gamma\gamma}$ ranges.

Range of $M_{\gamma\gamma}$ [GeV]	[65-119]	[85-100]	[94-100]
CMS data	170019	38159	13374
SM	171337	37986	16282
h' (BP1)	726	605	291
h (BP1)	549	167	79
h'+h+SM (BP1)	172612	38758	16652
h' (BP2)	472	396	185
h (BP2)	633	192	80
h'+h+SM (BP2)	172442	38574	16547
h' (BP3)	541	445	186
h (BP3)	550	167	79
h'+h+SM (BP3)	172428	38598	16547
h' (BP4)	717	583	124
h (BP4)	568	171	80
h'+h+SM (BP4)	172622	38740	16486
h' (BP5)	533	449	16498
h (BP5)	575	174	134
h'+h+SM (BP5)	172445	38609	82

considered five BPs and showed that each of these can produce an enhancement of the di-photon cross section in the above mass region through the subprocess $gg \to h' \to \gamma\gamma$ compatible with the CMS anomalous data while simultaneously producing the required amount of signal induced in the same channel by the SM-like state of the BLSSM, so as to comply with the di-photon data collected around 125 GeV. We also estimated the required integrated luminosity needed for a 5σ

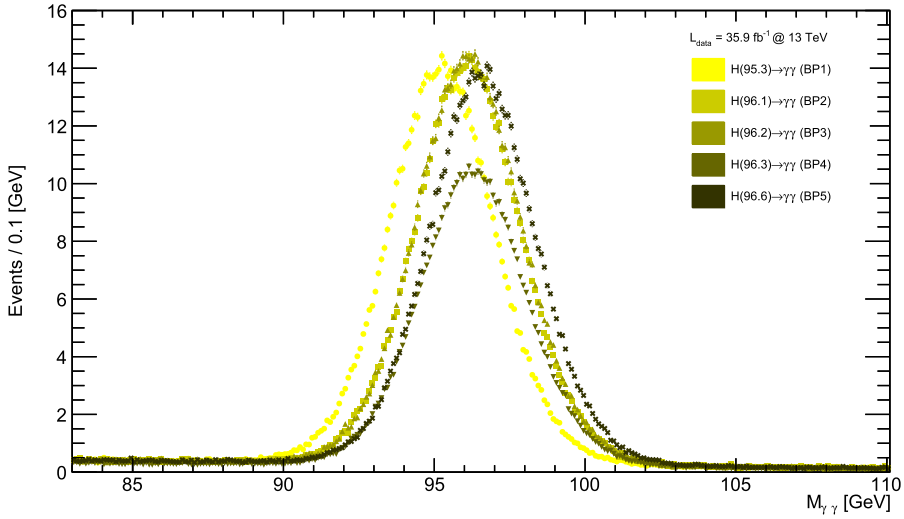

Fig. 8. Reconstructed h' mass distribution for all BPs with a bin width of 0.1 GeV.

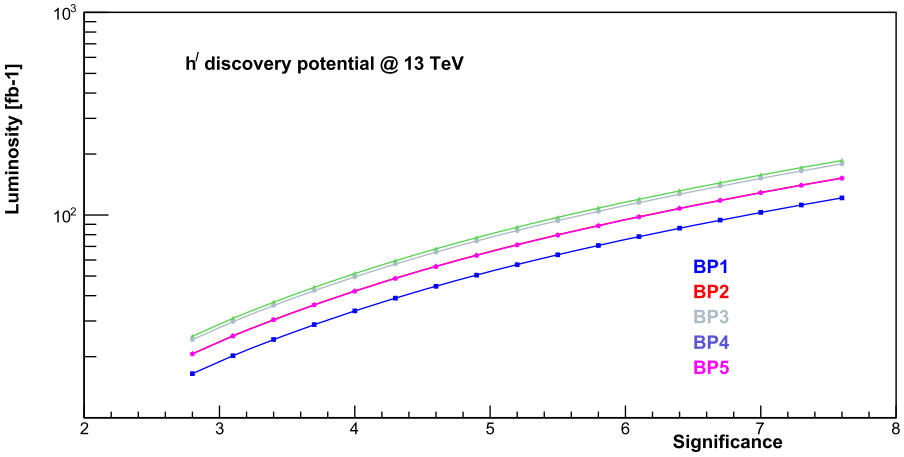

Fig. 9. Integrated luminosity needed for h' discovery in the di-photon channel as a function of significance for BP1–5.

discovery of such h' state in the above channel, which turned out to be less than the total Run 2 data sample, so that we advocate new analyses using the latter.

Declaration of competing interest

The authors declare the following financial interests/personal relationships which may be considered as potential competing interests: A. A. Abdelalim reports financial support was provided by Science and Technology Development Fund (grant number 37272). S. Khalil reports financial support was provided by Science and Technology Development Fund (grant number 37272). B. Das reports financial support was provided by Abdus Salam International Centre for Theoretical Physics (EAIFR). S. Moretti reports financial support was provided by NExT.

Data availability

Experimental Data used was taking from CMS published paper and the simulated data was made by the authors.

Acknowledgements

BD acknowledges the financial support provided by ICTP-EAIFR where part of this project was carried out. SM is financed in part through the NExT Institute and STFC Consolidated Grant No. ST/L000296/1. AA and SK work supported by Science, Technology & Innovation Funding Authority (STDF) under grant number 37272.

References

[1] S. Khalil, S. Moretti, Supersymmetry Beyond Minimality: from Theory to Experiment, CRC Press, Taylor & Francis Group, Boca Raton, FL, 2019.
[2] T. Aaltonen, et al., CDF, Science 376 (6589) (2022) 170–176;
B. Abi, et al., Muon g-2, Phys. Rev. Lett. 126 (14) (2021) 141801;
G. Arcadi, A. Djouadi, arXiv:2204.08406 [hep-ph].
[3] C. Han, K. Hikasa, L. Wu, J.M. Yang, Y. Zhang, Phys. Lett. B 769 (2017) 470.
[4] A.M. Sirunyan, et al., CMS, Phys. Lett. B 793 (2019) 320.
[5] W.G. Hollik, S. Liebler, G. Moortgat-Pick, S. Paßehr, G. Weiglein, Eur. Phys. J. C 79 (2019) 75;
F. Domingo, S. Heinemeyer, S. Paßehr, G. Weiglein, Eur. Phys. J. C 78 (2018) 942;
C. Beskidt, W. de Boer, D.I. Kazakov, Phys. Lett. B 782 (2018) 69;
K. Choi, S.H. Im, K.S. Jeong, C.B. Park, Eur. Phys. J. C 79 (2019) 956;
J. Cao, X. Guo, Y. He, P. Wu, Y. Zhang, Phys. Rev. D 95 (2017) 116001;
J. Cao, X. Jia, Y. Yue, H. Zhou, P. Zhu, Phys. Rev. D 101 (2020) 055008;
T. Biekötter, S. Heinemeyer, C. Muñoz, Eur. Phys. J. C 78 (2018) 504;
T. Biekötter, S. Heinemeyer, C. Muñoz, Eur. Phys. J. C 79 (2019) 667.
[6] P.J. Fox, N. Weiner, J. High Energy Phys. 08 (2018) 025;
U. Haisch, A. Malinauskas, J. High Energy Phys. 03 (2018) 135;
T. Biekötter, M. Chakraborti, S. Heinemeyer, Eur. Phys. J. C 80 (2020) 2;
T. Biekötter, M. Chakraborti, S. Heinemeyer, PoS CORFU2018 (2019) 015;
A. Kundu, S. Maharana, P. Mondal, Nucl. Phys. B 955 (2020) 115057.
[7] S. Khalil, S. Moretti, Front. Phys. 1 (2013) 10;
L. Basso, A. Belyaev, S. Moretti, G.M. Pruna, C.H. Shepherd-Themistocleous, PoS EPS-HEP2009 (2009) 242;
L. Basso, A. Belyaev, S. Moretti, G.M. Pruna, J. Phys. Conf. Ser. 259 (2010) 012062;
L. Basso, S. Moretti, G.M. Pruna, Phys. Rev. D 83 (2011) 055014;
W. Emam, S. Khalil, Eur. Phys. J. C 52 (2007) 625;
S. Khalil, J. Phys. G 35 (2008) 055001.
[8] ATLAS Collaboration, CERN Report No. ATLAS-CONF-2018-025, 2018.
[9] R. Barate, et al., LEP Working Group for Higgs Boson Searches, ALEPH, DELPHI, L3, OPAL, Phys. Lett. B 565 (2003) 61;
S. Schael, et al., ALEPH, DELPHI, L3, OPAL, LEP Working Group for Higgs Boson Searches, Eur. Phys. J. C 47 (2006) 547.
[10] S. Khalil, A. Masiero, Phys. Lett. B 665 (2008) 374.
[11] A. Hammad, S. Khalil, S. Moretti, Phys. Rev. D 92 (2015) 095008;
A. Hammad, S. Khalil, S. Moretti, Phys. Rev. D 93 (2016) 115035.
[12] W. Porod, Comput. Phys. Commun. 153 (2003) 275;
W. Porod, F. Staub, Comput. Phys. Commun. 183 (2012) 2458.
[13] F. Staub, Adv. High Energy Phys. 2015 (2015) 840780.
[14] G. Aad, et al., ATLAS, CMS, Phys. Rev. Lett. 114 (2015) 191803.
[15] P. Bechtle, O. Brein, S. Heinemeyer, G. Weiglein, K.E. Williams, Comput. Phys. Commun. 181 (2010) 138;
P. Bechtle, O. Brein, S. Heinemeyer, G. Weiglein, K.E. Williams, Comput. Phys. Commun. 182 (2011) 2605;

P. Bechtle, O. Brein, S. Heinemeyer, O. Stål, T. Stefaniak, G. Weiglein, K.E. Williams, Eur. Phys. J. C 74 (2014) 2693;
P. Bechtle, D. Dercks, S. Heinemeyer, T. Klingl, T. Stefaniak, G. Weiglein, J. Wittbrodt, Eur. Phys. J. C 80 (2020) 1211.
[16] P. Bechtle, S. Heinemeyer, O. Stål, T. Stefaniak, G. Weiglein, Eur. Phys. J. C 74 (2014) 2711;
O. Stål, T. Stefaniak, PoS EPS-HEP2013 (2013) 314;
P. Bechtle, S. Heinemeyer, O. Stål, T. Stefaniak, G. Weiglein, J. High Energy Phys. 11 (2014) 039;
P. Bechtle, S. Heinemeyer, T. Klingl, T. Stefaniak, G. Weiglein, J. Wittbrodt, Eur. Phys. J. C 81 (2021) 145.
[17] Y.S. Amhis, et al., HFLAV, arXiv:1909.12524 [hep-ex].
[18] J. Alwall, M. Herquet, F. Maltoni, O. Mattelaer, T. Stelzer, J. High Energy Phys. 06 (2011) 128.
[19] R.V. Harlander, S. Liebler, H. Mantler, Comput. Phys. Commun. 184 (2013) 1605.
[20] S. Catani, L. Cieri, D. de Florian, G. Ferrera, M. Grazzini, J. High Energy Phys. 04 (2018) 142.
[21] A.M. Sirunyan, et al., CMS, J. High Energy Phys. 11 (2018) 185.